Whole Brain White Matter Histogram Analysis of Diffusion Tensor Imaging Data Detects Microstructural Damage in Mild Cognitive Impairment and Alzheimer's Disease Patients

Giovanni Giulietti, MPhys,[1]* Mario Torso, PhD,[1] Laura Serra, PhD,[1] Barbara Spanò, PhD,[1] Camillo Marra, MD,[2] Carlo Caltagirone, MD,[3,4] Mara Cercignani, PhD,[1,5] Marco Bozzali, MD,[1] and the Alzheimer's Disease Neuroimaging Initiative (ADNI)

Background: Amnestic mild cognitive impairment (MCI) is a transitional stage between normal aging and Alzheimer's disease (AD). However, the clinical conversion from MCI to AD is unpredictable. Hence, identification of noninvasive biomarkers able to detect early changes induced by dementia is a pressing need.
Purpose: To explore the added value of histogram analysis applied to measures derived from diffusion tensor imaging (DTI) for detecting brain tissue differences between AD, MCI, and healthy subjects (HS).
Study Type: Prospective.
Population/Subjects: A local cohort (57 AD, 28 MCI, 23 HS), and an Alzheimer's Disease Neuroimaging Initiative (ADNI) cohort (41 AD, 58 MCI, 41 HS).
Field Strength: 3T. Dual-echo turbo spin echo (TSE); fluid-attenuated inversion recovery (FLAIR); modified-driven-equilibrium-Fourier-transform (MDEFT); inversion-recovery spoiled gradient recalled (IR-SPGR); diffusion tensor imaging (DTI).
Assessment: Normal-appearing white matter (NAWM) masks were obtained using the T_1-weighted volumes for tissue segmentation and T_2-weighted images for removal of hyperintensities/lesions. From DTI images, fractional anisotropy (FA), mean diffusivity (MD), axial diffusivity (AXD), and radial diffusivity (RD) were obtained. NAWM histograms of FA, MD, AXD, and RD were derived and characterized estimating: peak height, peak location, mean value (MV), and quartiles (C25, C50, C75), which were compared between groups. Receiver operating characteristic (ROC) and area under ROC curves (AUC) were calculated. To confirm our results, the same analysis was repeated on the ADNI dataset.
Statistical Tests: One-way analysis of variance (ANOVA), post-hoc Student's *t*-test, multiclass ROC analysis.
Results: For the local cohort, C25 of AXD had the maximum capability of group discrimination with AUC of 0.80 for "HS vs. patients" comparison and 0.74 for "AD vs. others" comparison. For the ADNI cohort, MV of AXD revealed the maximum group discrimination capability with AUC of 0.75 for "HS vs. patients" comparison and 0.75 for "AD vs. others" comparison.
Data Conclusion: AXD of NAWM might be an early marker of microstructural brain tissue changes occurring during the AD course and might be useful for assessing disease progression.
Level of Evidence: 1
Technical Efficacy: Stage 2

J. MAGN. RESON. IMAGING 2017;00:000–000.

View this article online at wileyonlinelibrary.com. DOI: 10.1002/jmri.25947

Received Apr 27, 2017, Accepted for publication Dec 21, 2017.

*Address reprint requests to: G.G., Santa Lucia Foundation, Via Ardeatina 306, 00179 Rome, Italy. E-mail: giulietti.giovanni@gmail.com

From the [1]Neuroimaging Laboratory, IRCCS Santa Lucia Foundation, Rome, Italy; [2]Institute of Neurology, Catholic University, Rome, Italy; [3]Department of Systemic Medicine, University of Tor Vergata, Rome, Italy; [4]Clinical and Behavioral Neurology Laboratory, IRCCS Santa Lucia Foundation, Rome, Italy; and [5]Department of Neuroscience, Clinical Imaging Sciences Centre, Brighton and Sussex Medical School, University of Sussex, Brighton, East Sussex, UK

Amnestic mild cognitive impairment (MCI) is regarded as a transitional stage between normal aging and fully developed Alzheimer's disease (AD).[1] However, the short-term clinical conversion from MCI to AD remains largely unpredictable. The identification of noninvasive biomarkers with the ability of staging MCI patients is becoming more and more critical for patients' management and clinical trials. While the standard diagnostic criteria for MCI are based on clinical/neuropsychological assessment,[1] several biomarkers,[2] have been proposed to improve diagnostic accuracy, such as medial temporal lobe atrophy,[3] positron emission tomography (PET) imaging measures such as beta-amyloid plaque load and index of cerebral glucose metabolism,[4,5] and cerebrospinal fluid (CSF) levels of beta-amyloid and phospho-tau.[6] However, medial temporal lobe atrophy has been shown not to be an early biomarker, being not evident in the asymptomatic stage of AD,[7] while CSF assessment is an invasive procedure and PET imaging requires the injection of a radioactive tracer that could present side effects (eg, allergic reaction). A large body of literature has demonstrated that white matter (WM) damage is present since the early clinical stages of AD, and strongly contributes to the disease progression.[8]

Diffusion tensor imaging (DTI) is one of the preferred magnetic resonance imaging (MRI) methods for WM investigation in vivo, detecting macro- and microscopic tissue abnormalities.[9] To date, several DTI-derived indices (eg, fractional anisotropy [FA], mean diffusivity [MD], axial [AXD], and radial diffusivity [RD]) have been proposed as reflecting different aspects of WM microstructure and damage.[10] Against this background it is conceivable that these different DTI parameters may change differently across AD evolution, possibly reflecting different aspects of AD pathophysiology (eg, axonal damage and loss, demyelination, etc.).

Histogram analysis has been largely used to analyze data coming from MRI for the investigation of various neurological disorders.[11–13] This approach offers the advantage, compared to region of interest or voxel-based analyses, of being operator-independent and of summarizing the information from a whole image into a few simple numerical indices.

The principal aim of this study was to define the evolution of WM damage as assessed by different DTI-based histogram parameters at different AD stages. The secondary aim was to identify the most promising prognostic parameter (or set of parameters) to be used in clinical settings.

Materials and Methods

Subjects

This prospective study was approved by the local Ethics Committee and written informed consent was obtained from all participants before the study initiation.

One hundred patients were recruited from the Specialist Dementia Clinics of our institution (Table 1). Fifteen patients were excluded for the following reasons: 1) claustrophobia or poor cooperation during MRI, with scanning interruption before completing the protocol acquisition ($n = 7$); and 2) the presence of artifacts on MR images ($n = 8$). Out of the 85 enrolled patients, 57 fulfilled the diagnostic criteria for AD and 28 those of amnestic MCI, as defined below. The diagnosis of AD was made according to the National Institute of Neurological and Communication Disorders and Stroke/Alzheimer's Disease and Related Disorders Association criteria (NINCDS-ADRDA).[14] AD patients also had to fulfill the Diagnostic and Statistical Manual of Mental Disorders (DSM-5) criteria for major neurocognitive disorders.[15]

MCI patients had to show episodic memory disorders[1] and no or very mild impairment in daily living activities, with a total Clinical Dementia Rating score not exceeding 0.5.[16] Within 3 days after recruitment, patients underwent neuropsychological and behavioral assessments and an MRI scan. With respect to the presence and severity of macroscopic WM lesions, there are no definite cutoff criteria available to discriminate between vascular and neurodegenerative dementia. To reduce as much as possible the risk of including patients with vascular MCI, principal comorbidities (ie, diabetes, hypertension, hyperlipidemia, arrhythmias) and risk factors (ie, alcohol abuse) for developing cerebrovascular pathology were ruled out in all patients. Additionally, in every patient, the Hachinski score,[17] a clinical tool often used to differentiate between AD and vascular dementia, had to be less than 4, and the total WM lesion volume had not to exceed 25 ml.[18]

Twenty-three healthy elderly subjects (HS) were also recruited from the relatives of patients and served as a control group (Table 1). All HS with major systemic and neurological illnesses, cognitive deficits, and Behavioral and Psychological Symptoms of Dementia (BPSD) were excluded. Finally, to reduce any potential source of variability due to hemispheric dominance, all subjects had to be right-handed, as assessed by the Edinburgh Handedness Inventory.[19] From now on, we refer to this group of 108 subjects as the *local cohort*.

Neuropsychological Assessment (Local Cohort)

All subjects of the local cohort underwent a neuropsychological battery, including the following tests: verbal episodic long-term memory: 15-Word List (Immediate and 15-min Delayed recall)[20] and Short Story Test (Immediate and 20-min Delayed recall)[20]; visuospatial episodic long-term memory: Complex Rey's Figure (Immediate and 20-min Delayed recall)[20]; short-term memory: Digit span and the Corsi Block Tapping task[21]; executive functions: Phonological Word Fluency[20] and Modified Card Sorting Test[20]; language: Naming objects subtest of the BADA (Batteria per l'Analisi dei Deficit Afasici)[22]; reasoning: Raven's Coloured Progressive Matrices[20]; constructional praxis: Copy of simple drawings with and without landmarks,[20] and Copy of Complex Rey's Figure[20]; general cognitive efficiency: Mini-Mental State Examination (MMSE).[20,23] For all employed tests, we used the Italian normative data for both score adjustment (sex, age, and education) and to define cutoff scores of normality, determined as the lower limit of the 95% tolerance interval for a confidence level of 95%.

TABLE 1. Principal Demographic and Clinical Characteristics of the Participants Belonging to the Local (Upper Numbers) and *ADNI* (*Lower Numbers*) Cohorts

	AD	MCI	HS	*P*-value AD vs. MCI	*P*-value AD vs. HS	*P*-value MCI vs. HS
N	57 *41*	28 *58*	23 *41*			
Age (years)	72.2 [6.6] *74.5 [8.5]*	70.9 [8.5] *72.2 [6.9]*	68.4 [6.9] *71.9 [6.1]*	ANOVA ns: 0.11 ANOVA ns: 0.18		
Female/male ratio	36/21 *15/26*	16/12 *20/38*	10/13 *23/18*	chi-square ns: 0.27 chi-square ns: 0.07		
Education (years)	9.2 [4.3][a] not available	9.9 [4.6] not available	12.2 [2.9] not available	0.302 /	**0.011** /	0.043 /
MMSE[c]	21.0 [3.9][a,b] *22.3 [3.6][a,b]*	26.8 [1.8][a] *27.0 [1.9][a]*	29.0 [1.0] *28.9 [1.1]*	**< 0.001** **< 0.001**	**< 0.001** **< 0.001**	**< 0.001** **< 0.001**
GM fraction	0.42 [0.02][a,b] *0.37 [0.03][a,b]*	0.43 [0.02] *0.40 [0.03][a]*	0.44 [0.01] *0.42 [0.02]*	**0.009** **0.002**	**< 0.001** **< 0.001**	0.053 **< 0.001**
NAWM fraction	0.31 [0.02] *0.29 [0.03][a,b]*	0.32 [0.02] *0.31 [0.02]*	0.32 [0.02] *0.31 [0.02]*	ANOVA ns: 0.33 **0.005**	**< 0.001**	0.249
WMHs fraction	0.003 [0.003] *0.003 [0.003]*	0.003 [0.004] *0.003 [0.002]*	0.001[0.002] *0.002 [0.002]*	ANOVA ns: 0.17 ANOVA ns: 0.10		

Unless otherwise noted, all values are expressed as mean [standard deviation]. All measures were compared between groups using Student's *t*-test. Bonferroni correction was used to account for multiple comparisons ($P < 0.05$). Statistically significant *P*-values are highlighted in bold. AD = Alzheimer's disease; GM = gray matter; HS = healthy subjects; MCI = mild cognitive impairment; MMSE = Mini-Mental State Examination (raw); NAWM = normal appearing white matter; WMHs = white matter hyperintensities; ns = not significant.
[a]Statistically significant difference between patients (AD or MCI) and HS.
[b]Statistically significant difference between AD and MCI.
[c]Due to lack of data in ADNI database, mean values of MMSE in ADNI cohort were computed in only 30 out of 41 AD, 49 out of 58 MCI and 36 out of 41 HS (115 out of 140 subjects).

For each test, normative data are reported in the corresponding references.

MRI Data Acquisition (Local Cohort)

All subjects of the local cohort underwent MRI scanning at 3T (Magnetom Allegra, Siemens, Erlangen, Germany), including the following acquisitions: 1) dual-echo turbo spin echo (dual-echo TSE, repetition time [TR] = 7600 msec, echo time [TE] = 12/109 msec, matrix = 256 × 192, field of view [FOV] = 230 × 172.5 mm^2, slice thickness 3 mm); 2) fast-fluid-attenuated inversion recovery (FLAIR; TR = 8170 msec, TE = 96 msec, inversion time [TI] = 2100 msec, same matrix, FOV, and slice thickness as the TSE); 3) 3D modified-driven-equilibrium-Fourier-transform (MDEFT; TR = 1394 msec, TE = 2.4 msec, TI = 910 msec, matrix = 256 × 224 × 176, in-plane FOV = 256 × 224 mm^2, slice thickness = 1 mm); 4) diffusion-weighted (DW) twice-refocused spin-echo echo planar imaging (SE EPI; TR = 10.2 sec, TE = 85 msec, b factor = 1000 s/mm^2, isotropic resolution = 2.3 mm^3). This last sequence collects seven images with no diffusion weighting (b_0) and 61 images with diffusion gradients applied in 61 noncollinear directions.

Image Processing and Histogram Analysis (Local Cohort)

BRAIN TISSUE SEGMENTATION. White matter hyperintensities (WMHs) were identified by consensus of two trained observers (with 3 and 10 years of experience in head imaging analysis, respectively) on the T_2-weighted image (the longest echo time image of sequence[1]), using semiautomated local thresholding contouring software (Jim 4.0, Xinapse System, Leicester, UK, http://www.xinapse.com/). FLAIR images were used to increase confidence in lesion identification.

Binary lesion masks and lesion volumes were then calculated. The T_2-weighted images were then affine-registered to the

T_1-weighted images (MDEFT) using ANTs.[24] The same transformation parameters were applied to the lesion mask. Then lesions were stripped from the T_1-weighted images, which were then processed using SPM8 (www.fil.ion.ucl.ac.uk/spm/) toolbox VBM8 (www.neuro.uni-jena.de/vbm/download/) to yield local volumes maps of gray matter (GM), normal-appearing white matter (NAWM), and CSF. These maps were used to compute global brain tissues volumes (GMvol, NAWMvol, CSFvol). To account for subjects' head size differences, the global brain tissue volumes were expressed as percentages of the total intracranial volume (ICV = GMvol+NAWMvol+WMHs_vol+CSFvol), by computing GM fraction (GMvol/ICV), NAWM fraction (NAWMvol/ICV), and lesion fraction (WMHs_vol/ICV). These measures were obtained to further characterize the patient groups included in the study and ensure consistency with previously reported cohorts.

DTI ANALYSIS. DW images were processed using tools from the FMRIB software library (FSL, http://fsl.fmrib.ox.ac.uk/fsl/fslwiki/) and CAMINO (http://camino.cs.ucl.ac.uk/).

First, diffusion data were corrected for misalignment between volumes according to the following steps:

1. the seven b_0 images were realigned to the first b_0 volume with a rigid body transformation and averaged (obtaining $meanb_0$);
2. the seven b_0 images were rigidly coregistered to $meanb_0$;
3. the 61 DW volumes were averaged obtaining meanDW; meanDW was then rigidly coregistered to the scalp stripped $meanb_0$ image through the transformation T_1;
4. all DW volumes (i = 1, 2, . . ., 61) were separately realigned to the meanDW image (with a rigid body transformation, $T\_2^{(i)}$), and the transformation matching each DW volume with the $meanb_0$ image was obtained by combining $T\_2^{(i)}$ and T_1.

The b matrices were rotated accordingly.[25] The final realigned DW volumes were obtained by merging the images from steps 2 and 4. Therefore, the diffusion tensor was estimated in every voxel and maps of FA, MD, RD, and AXD were obtained for each subject.

HISTOGRAM COMPUTATION AND FEATURES EXTRACTION. For all participants, T_1-weighted images were warped to the FA map using ANTs[24]; the same nonlinear transformation was then applied to the NAWM mask. This way we could create histograms of each DTI measure (FA, MD, AXD, RD) distribution in the NAWM (four histograms per subject).

An absolute histogram was created by dividing the full range of image intensity into a number of bins, each spanning a fraction of the full range and counting the number of voxels with a value falling in each bin. Absolute NAWM histograms were computed using 0.5% of the maximum wide bins (200 bins). Absolute histograms were then normalized, dividing by both the bin width and the total number of voxels contributing to the histogram. The effect of normalization is to make the shape of the histograms independent from the brain size.[26] Histograms were analyzed following guidelines available in Ref. 26, using in-house MatLab (MathWorks, Natick, MA) scripts. To increase the reliability of peak detection, the histograms of NAWM were smoothed using an 8^{th} order median filter. Next, from each normalized and smoothed histogram, we derived: peak height (PH), peak location (PL), 25^{th} centile (C25), 50^{th} centile (C50), 75^{th} centile (C75), and mean value (MV). These six parameters are able to appropriately characterize histograms with unimodal shape.[26]

Repeated Analysis on the ADNI Cohort

In order to test if the results obtained in the local cohort were independent from both scanner and clinical evaluation for patients' dementia staging, we replicated all the analyses using a completely different dataset, obtained from the Alzheimer's Disease Neuroimaging Initiative (ADNI, http://adni.loni.usc.edu). ADNI is a global research effort that actively supports the investigation and development of treatments that slow or stop the progression of AD; in this view, ADNI makes publicly available neuropsychological (including MMSE) and imaging data for HS, early MCI (EMCI), late MCI (LMCI), and AD patients, often including different timepoints per subject (longitudinal data).

From the ADNI database, we downloaded data relative to subjects whose MRI protocol included at least T_1 3D, DTI, and FLAIR sequences (not available, dual-echo TSE); if there were more than one MRI dataset per subject (longitudinal acquisitions), we selected the oldest timepoint for which the MMSE score was available. In every patient the total WM lesion volume, as assessed from FLAIR images, did not exceed 25 ml.[18] Using these constraints, we were able to collect data including 41 HS, 58 MCI (27 EMCI, 31 LMCI), and 41 AD. We refer to this dataset of 140 subjects as the *ADNI cohort*, whose main demographic characteristics are given in Table 1.

MRI Data Acquisition (ADNI Cohort)

MRI data for the ADNI cohort were collected at several sites, all equipped with a whole-brain 3T MRI scanner (GE Medical Systems, Milwaukee, WI). The protocol included: 1) fast-fluid-attenuated inversion recovery (FLAIR; TR = 11,000 msec, TE = 150 msec, TI = 2250 msec, matrix = 256 × 256, FOV = 220 × 220 mm^2, slice thickness = 5 mm); 2) inversion-recovery spoiled gradient recalled T_1-weighted (IR-SPGR; TR = 1422 msec, TE = 3 msec, TI = 400 msec, matrix = 256 × 256 × 196; in-plane FOV = 260 × 260 mm^2, slice thickness = 1.2 mm); 3) DW twice-refocused spin-echo echo planar imaging (TR = 13 sec, TE = 70 msec, b factor = 1000 s/mm^2, voxel size = 1.37 × 1.37 × 2.7 mm^3). This last sequence collects five images with no diffusion weighting and 41 diffusion-weighted images.

Image Processing and Histogram Analysis (ADNI Cohort)

Brain tissue segmentation, DTI analysis, and histogram computation were performed following the same pipelines described for the local cohort.

Statistical Analysis

Statistical analysis was performed using the Statistics Toolbox available in MatLab. In all the analyses of variance (ANOVAs) and post-hoc Student's *t*-tests, we set the statistical significance threshold to $P = 0.05$ and then applied the Bonferroni correction for multiple comparisons. The same analyses were performed for both local and ADNI cohorts.

All demographic characteristics but female/male ratio, clinical characteristics, and brain tissue volumetrics were compared between all groups (HS, AD, MCI) using a one-way ANOVA; on the measures surviving the ANOVA analysis, post-hoc Student's *t*-tests were performed. The female/male ratios were compared between groups using a chi-square test, considering as significant $P < 0.05$. For the local cohort, the neuropsychological scores (not available in the ADNI cohort) were compared between all groups using a one-way ANOVA; on the scores surviving the ANOVA analysis, post-hoc Student's *t*-tests were performed.

MULTICLASS ROC ANALYSIS OF HISTOGRAM-DERIVED FEATURES. The six histogram-derived indices (PH, PL, C25, C50, C75, MV) relative to FA, MD, AXD, and RD in NAWM were compared between groups using a one-way ANOVA. On the indices surviving the ANOVA analysis, post-hoc Student's *t*-tests were performed. In the ANOVA and *t*-test analyses, we considered as significant $P < 0.05$, applying the Bonferroni correction for multiple comparisons (we set the statistical threshold to 0.05/24 in the ANOVA analysis, and to 0.05/3 in the post-hoc *t*-tests).

To assess the capability of group discrimination of each histogram-derived index, we employed a multiclass receiver operating characteristic (ROC) curve analysis. ROC analysis is typically used for two-groups diagnostic problems.[27] In our case (three groups) we used the multiclass problem approach. One method for handling $n > 2$ classes is to produce n different ROC curves, one for each class. In particular, the ROC curve for class j (with j spanning from 1 to n) refers to the classification performance in which j is the positive class and all other n-1 classes are combined to form the negative class.[27] While this approach can be straightforwardly applied to n mutually independent classes, the three classes involved in this study (HS, MCI, AD) do not fulfill this criterion, MCI being a prodromal stage of AD. Consequently, the comparison of MCI vs. HS plus AD is meaningless and was not modeled. We thus retained only the two class comparisons "MCI plus AD vs. HS," and "AD vs. HS plus MCI." For each comparison we considered the feature with the highest AUC (area under the ROC curve) as the "best discriminator."

POST-HOC CORRELATION ANALYSIS. In the patients group only, Spearman partial correlation (controlled for age, gender, and education) was used to test for associations between general cognitive efficiency (measured by the MMSE score) and the "best discriminator" histogram features as revealed by ROC analyses. $P < 0.05$ was considered statistically significant.

Results

Demographic and Neuropsychological Data

Demographic and clinical characteristics of the studied subjects are summarized in Table 1.

Local Cohort: According to the inclusion criteria, there were no significant differences in age ($F_{2,105} = 2.26$, $P = 0.11$) or gender distribution (chi-square = 2.60, $P = 0.27$) between the groups. Conversely, there were differences in years of formal education ($F_{2,105} = 4.61$, $P = 0.012$), resulting AD patients being less educated than HS. As expected, the three groups showed significantly different MMSE scores ($F_{2,105} = 67.77$, $P < 0.0001$). From a neuropsychological viewpoint, MCI patients performed worse than HS at tests exploring long-term verbal episodic memory and verbal and visuospatial short-term memory. Moreover, MCI patients reported significantly lower scores than HS in the Modified Card Sorting Test. Patients with AD reported a widespread cognitive impairment involving all domains (Table 2).

ADNI Cohort: There were no significant group differences with respect to age ($F_{2,137} = 1.72$, $P = 0.18$) and gender distribution (chi-square = 5.19, $P = 0.07$), while MMSE scores (available for 115 out of 140 subjects) were significantly different ($F_{2,112} = 38.43$, $P < 0.0001$) across groups (Table 1).

Brain Tissue Volumetrics

Brain volumetrics of all subjects are summarized in Table 1.

Local Cohort: AD patients showed a significantly lower GM fraction than MCI patients and HS ($F_{2,105} = 14.04$, $P < 0.0001$). When comparing MCI patients to HS, no significant difference was found. No differences in NAWM fraction were detected between any of the groups ($F_{2,105} = 1.12$, $P = 0.33$). Although the average lesion fraction was higher in both patients group compared to HS, these differences were not statistically significant ($F_{2,105} = 1.79$, $P = 0.17$).

ADNI Cohort: GM fractions were different in each group ($F_{2,137} = 37.20$, $P < 0.0001$). AD patients also showed a significantly lower NAWM fraction than MCI patients and HS ($F_{2,137} = 8.07$, $P < 0.0001$); when comparing MCI patients to HS, no significant difference was found. The average lesion fractions were not significant different between groups ($F_{2,137} = 2.38$, $P = 0.10$).

Histograms Computation

Local Cohort: With the exception of FA, all NAWM histograms had a clear unimodal shape for all participants (Fig. 1A). The FA histograms, in several subjects, presented instead a maximum with a plateau or two maxima with similar height and close to each other. For this reason, for the FA histograms we computed C25, C50, C75, and MV, but not PH and PL.

ADNI Cohort: For all subjects, all NAWM histograms had a clear unimodal shape (Fig. 1B).

Multiclass ROC Analysis of Histogram-Derived Features

Local Cohort: No between-group difference was found in PH, PL, and C75 of MD, AXD, and RD. Both patient groups, compared to HS, showed higher C25, C50, and MV relative to MD, AXD, and RD. AD compared to MCI patients showed a significant increase in C25 of AXD histogram ($C25_{AXD}$). No between-group difference was found in any of the FA histogram-derived metrics (Table 3). The

TABLE 2. Performance Obtained by Patients and Healthy Control Subjects (Belonging to the Local Cohort) on Neuropsychological Testing

Cognitive domain	Neuropsychological test	AD (n = 57)	MCI (n = 28)	HS (n = 23)
Verbal episodic Long-term memory				
	15-Words List:			
	Immediate recall (cutoff $\geq$ 28.5)	23.2 (9.1)[a,b]	29.9 (5.8)[a]	45.8 (8.8)
	Delayed recall (cutoff $\geq$ 4.6)	2.5 (2.4)[a,b]	4.5 (2.3)[a]	9.4 (2.0)
	Short story test:			
	Immediate recall (cutoff $\geq$3.1)	2.2 (2.0)[a,b]	4.6 (1.3)	6 (1.4)
	Delayed recall (cutoff $\geq$ 2.6)	0.9 (1.8)[a,b]	3.7 (2.2)[a]	5.9 (1.2)
Visuo-spatial episodic long-term memory				
	Complex Rey's Figure:			
	Immediate recall (cutoff $\geq$ 6.4)	5.6 (5.2)[a,b]	10.9 (6.6)	14.2 (7.9)
	Delayed recall (cutoff $\geq$ 6.3)	4.7 (5.1)[a,b]	9.5 (7.1)[a]	14.3 (6.2)
Verbal Short-term memory				
	Digit span (cutoff $\geq$ 3.7)	4.7 (1.2)[a]	5.2 (0.9)	5.9 (1.1)
Visuo-spatial Short-term memory				
	Corsi span (cutoff $\geq$ 3.5)	3.6 (1.3)[a,b]	4.3 (0.6)	5 (0.9)
Executive functions				
	Phonological Word Fluency (cutoff $\geq$17.3)	26.8 (8.2)[a]	31.8 (7.3)	36.6 (8.8)
	Modified Card Sorting Test Criteria achieved (cutoff $\geq$ 4.2)	2.4 (1.7)[a,b]	3.7 (1.9)[a]	5.7 (0.8)
	Modified Card Sorting Test Perseverative errors (cutoff $\leq$7.6)	11.3 (11.5)[a]	6.6 (4.9)	1.9 (3.5)
Language				
	Naming of objects (cutoff $\geq$ 22)	24.4 (5.6)	28.4 (1.6)	29.1 (0.9)

TABLE 2: Continued

Cognitive domain	Neuropsychological test	AD (n = 57)	MCI (n = 28)	HS (n = 23)
Reasoning				
	Raven's Colored Progressive Matrices (cutoff $\geq$ 18.9)	22.9 (6.3)[a,b]	27.7 (4.7)[a]	32.6 (2.8)
Constructional praxis				
	Copy of drawings (cutoff $\geq$ 7.1)	7.4 (3.3)[a,b]	9.4 (1.7)	10.7 (1.3)
	Copy of drawings with landmarks (cutoff $\geq$ 61.8)	56.7 (16.4)[a,b]	66 (4.4)	69.3 (0.9)
	Copy of Complex Rey's Figure (cutoff $\geq$ 23.7)	20.5 (12.5)[a,b]	29.8 (6.7)	32.6 (2.1)

All values are expressed as: mean (SD). All measures were compared between groups using Student's *t*-test. Bonferroni correction was used to account for multiple comparisons ($P < 0.05$). For each administered test appropriate adjustments for gender, age, and education were applied according to the Italian normative data. Available cutoff scores of normality (>95% of the lower tolerance limit of the normal population distribution) are also reported for each test. AD = Alzheimer's disease; HS = healthy subjects; MCI = mild cognitive impairment.
[a]Statistically significant difference between patients (AD or MCI) and HS.
[b]Statistically significant difference between AD and MCI.

ROC analyses were thus performed on the following indices: C25, C50, and MV of AXD, RD, and MD.

$C25_{AXD}$ was the best between-group discriminator, having a maximum AUC of 0.80 (95% confidence intervals [CI]: 0.65–0.95) for MCI plus AD vs. HS (Fig. 2A) and of 0.74 (95% CI: 0.60–0.88) for AD vs. HS plus MCI comparison (Fig. 3A).

ADNI Cohort: As in the local cohort, no between-group difference was found in any of the FA histogram-derived metrics. Both AD and MCI, compared to HS, showed higher C25, C50, C75, MV of AXD, C50, MV of MD, and MV of RD. AD compared to HS also showed lower PH of AXD and higher C75 of MD and RD. AD compared to MCI had lower PH of AXD and higher C75 and MV of AXD and MV of MD (Table 3). The ROC analyses were thus performed on the following indices: PH, C25, C50, C75, and MV of AXD, C50, C75, and MV of MD, and C75 and MV of RD.

MV_{AXD} was the best between-group discriminator, having a maximum AUC of 0.75 (95% CI: 0.62–0.87) for MCI plus AD vs. HS (Fig. 2B) and of 0.75 (95% CI: 0.63–0.87) for AD vs. HS plus MCI (Fig. 3B) comparison.

Post-Hoc Correlation Analysis

Local Cohort: In the patients group (MCI plus AD) we found a significant Spearman partial correlation (adjusted for age, gender, and education) equal to $r = -0.34$ ($P = 0.0016$) between MMSE raw score and $C25_{AXD}$.

ADNI Cohort: In the patients group (MCI plus AD) a significant Spearman partial correlation (adjusted for age and gender; education scores were not available) equal to $r = -0.30$ ($P = 0.0079$) between MMSE raw score and MV_{AXD} was found.

Discussion

In this study we assessed the ability of NAWM diffusivity changes to classify patients at different stages of the clinical course of AD and evaluated the suitability of histogram-derived metrics for patient staging and monitoring disease progression. Several previous studies attempted to define the features of diffusivity changes in the advanced stages of AD[28] and to identify correlations with clinical evaluations or measures of cognitive decline such as the MMSE score.[7] However, it remains to be clarified whether a simple quantification of DTI parameters can support patient staging.

In the current study we used histogram analysis, which is able to detect subtle global changes in the brain tissue and is particularly indicated when dealing with a diffuse disease such as AD.[29] Histograms summarize the information derived from large portions of tissue (in our case, the whole NAWM) into a curve, which can be characterized by simple metrics. In this work we compared the diagnostic reliability of a number of histogram metrics, computed for FA, MD, AXD, and RD.

Our study strongly suggests that the information delivered by AXD of NAWM is the most informative DTI

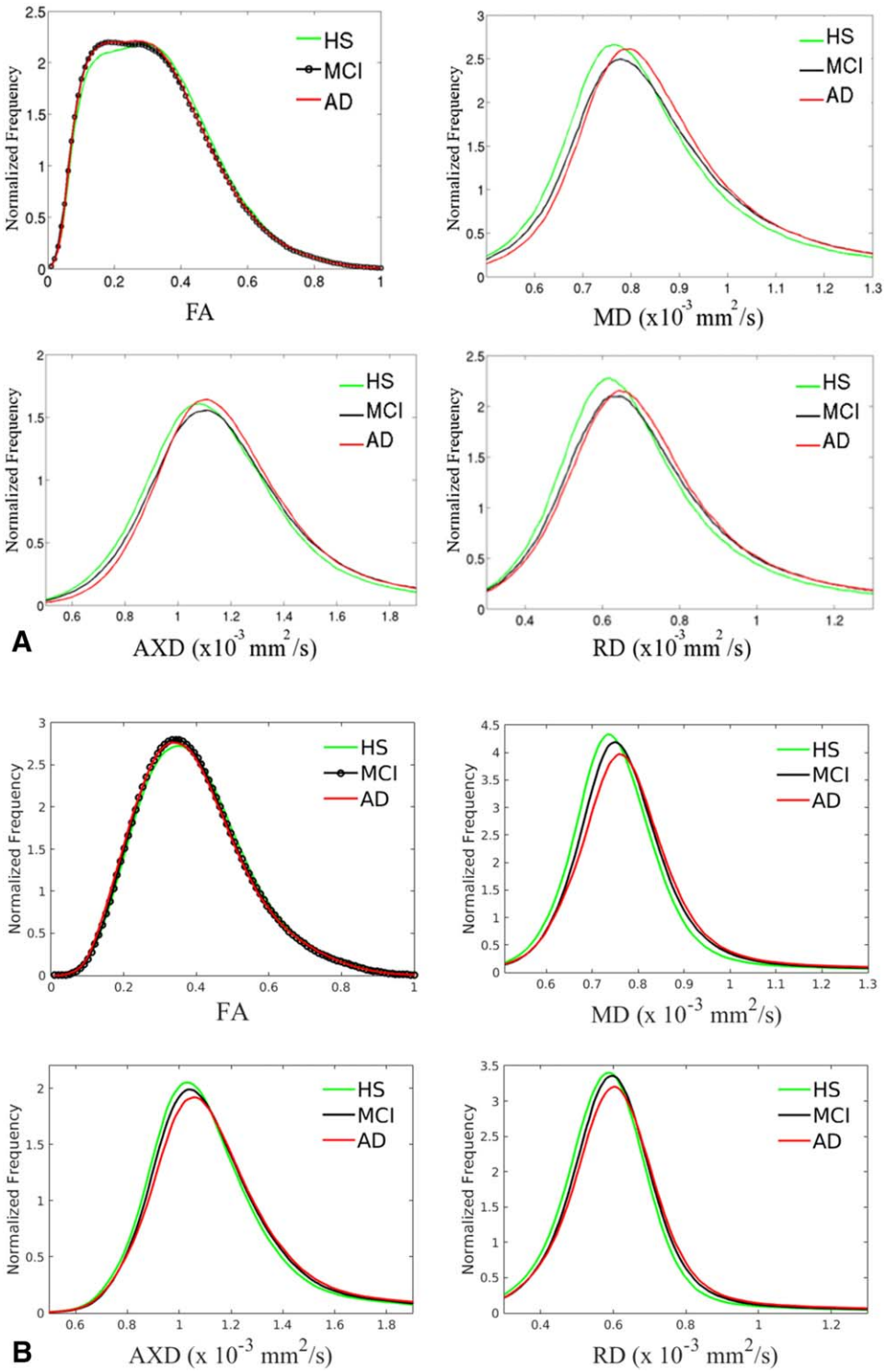

FIGURE 1: Group-averaged histograms of FA, MD, AXD, and RD in NAWM of three groups: HS (green), MCI (black) and AD patients (red). A: Local cohort dataset. B: ADNI cohort dataset.

measure regarding the biological evolution of AD in the human brain. The data analysis identically performed on a local dataset (108 subjects) and ADNI dataset (140 subjects) has indeed found in both cases that AXD histogram-related parameters had the best performance in distinguishing AD, MCI, and HS.

In particular, with the post-hoc *t*-test analysis we found that, for the local cohort dataset, C25, C50, MV of MD, AXD and RD were able to distinguish patients (MCI, AD) from healthy subjects. More interestingly, $C25_{AXD}$ was as the only parameter different in each group and the most sensitive parameter to differentiate either AD

TABLE 3. Histogram-Derived Indices of DTI Measures in NAWM of Patients (AD, MCI) and HS, for the Local (Upper Numbers) and *ADNI* (*Lower Numbers*) Cohorts

FA

	PH	PL	C25	C50	C75	MV
AD	/ *2.79 [0.16]*	/ *0.34 [0.02]*	0.18 [0.01] *0.27 [0.02]*	0.29 [0.02] *0.36 [0.02]*	0.42 [0.02] *0.47 [0.02]*	0.31 [0.02] *0.38 [0.02]*
MCI	/ *2.83 [0.15]*	/ *0.34 [0.03]*	0.18 [0.02] *0.28 [0.02]*	0.29 [0.02] *0.37 [0.02]*	0.42 [0.02] *0.47 [0.02]*	0.31 [0.02] *0.39 [0.02]*
HS	/ *2.75 [0.18]*	/ *0.35 [0.03]*	0.18 [0.02] *0.28 [0.01]*	0.30 [0.02] *0.37 [0.02]*	0.42 [0.02] *0.48 [0.02]*	0.32 [0.02] *0.39 [0.02]*

MD

	PH	PL	C25	C50	C75	MV
AD	2.75 [0.45] *4.14 [0.61]*	0.80 [0.03] *0.76 [0.03]*	0.75 [0.03][a] *0.71 [0.02]*	0.85 [0.04][a] *0.78 [0.03][a]*	1.00 [0.06] *0.85 [0.03][a]*	0.92 [0.04][a] *0.83 [0.03][a,b]*
MCI	2.63 [0.45] *4.55 [0.72]*	0.79 [0.04] *0.76 [0.03]*	0.74 [0.03][a] *0.71 [0.03]*	0.84 [0.04][a] *0.77 [0.03][a]*	1.00 [0.07] *0.84 [0.04]*	0.92[0.05][a] *0.81 [0.04][a]*
HS	2.78 [0.35] *4.61 [0.65]*	0.77 [0.03] *0.74 [0.03]*	0.72 [0.02] *0.69 [0.02]*	0.81 [0.03] *0.75 [0.03]*	1.00 [0.05] *0.82 [0.03]*	0.88 [0.04] *0.79 [0.03]*

AXD

	PH	PL	C25	C50	C75	MV
AD	1.67 [0.16] *1.95 [0.14][a,b]*	1.11 [0.04] *1.06 [0.03]*	1.01 [0.03][a,b] *0.98 [0.03][a]*	1.17 [0.04][a] *1.11 [0.03][a]*	1.36 [0.05] *1.29 [0.04][a,b]*	1.23 [0.04][a] *1.19 [0.04][a,b]*
MCI	1.59 [0.14] *2.04 [0.14]*	1.10 [0.04] *1.05 [0.04]*	0.99 [0.03][a] *0.97 [0.03][a]*	1.16 [0.04][a] *1.10 [0.04][a]*	1.36 [0.06] *1.27 [0.05][a]*	1.22 [0.05][a] *1.17 [0.04][a]*
HS	1.62 [0.10] *2.08 [0.12]*	1.08 [0.03] *1.03 [0.03]*	0.97 [0.03] *0.96 [0.02]*	1.13 [0.03] *1.08 [0.03]*	1.32 [0.04] *1.24 [0.03]*	1.18 [0.04] *1.14 [0.03]*

RD

	PH	PL	C25	C50	C75	MV
AD	2.25 [0.29] *3.30 [0.35]*	0.65 [0.04] *0.61 [0.03]*	0.58 [0.03][a] *0.53 [0.02]*	0.70 [0.04][a] *0.61 [0.03]*	0.87 [0.06] *0.70 [0.03][a]*	0.77[0.04][a] *0.66 [0.03][a]*
MCI	2.20 [0.29] *3.55 [0.41]*	0.64 [0.05] *0.60 [0.04]*	0.57 [0.04][a] *0.53 [0.03]*	0.69 [0.05][a] *0.60 [0.03]*	0.86 [0.07] *0.68 [0.04]*	0.77[0.05][a] *0.64 [0.04][a]*
HS	2.35 [0.22] *3.56 [0.33]*	0.62 [0.03] *0.59 [0.03]*	0.55 [0.04] *0.51 [0.03]*	0.67 [0.03] *0.59 [0.03]*	0.82 [0.05] *0.67 [0.03]*	0.73 [0.04] *0.62 [0.03]*

All values are expressed as: mean [SD]. Diffusivity measures are expressed in $10^{-3}mm^2/s$.
All indices were compared between groups using Student's *t*-test. Bonferroni correction was used to account for multiple comparisons ($P < 0.05$). AD = Alzheimer's disease; AXD = axial diffusivity; C25 = 25th centile of histogram; C50 = 50th centile of histogram; C75 = 75th centile of histogram; FA = fractional anisotropy; HS = healthy subjects; MCI = mild cognitive impairment; MD = mean diffusivity; MV = histogram mean value; NAWM = normal appearing white matter; PH = peak height of histogram; PL = peak location of histogram; RD = radial diffusivity.
[a]Statistically significant difference between patients (AD or MCI) and HS.
[b]Statistically significant difference between AD and MCI.

patients from the HS plus MCI group and HS from the MCI plus AD group, as demonstrated by ROC curves and AUC values.

Similarly, the analysis on the ADNI dataset has shown that MV of MD and AXD and C75 of AXD were all significantly different in each group, but the ROC analysis highlighted MV_{AXD} as the measure with the maximum AUC value in the two comparisons.

$C25_{AXD}$ and MV_{AXD} accounted also for the patients' level of global cognitive impairment of the two cohorts, as highlighted by the post-hoc correlation analysis.

It is meaningful that in two independent datasets we observed that AXD was the best discriminator between groups ($C25_{AXD}$ for local dataset and MV_{AXD} for ADNI dataset). In terms of histogram features, however, we found some differences between datasets. For the local dataset, C25 was the best discriminator, while for the ADNI dataset it was MV. We can speculate on the source of this inconsistency, bearing in mind that these features ultimately reflect the shape of the histograms, which in turn depend on the NAWM masks, on the DTI maps and on the anatomical to DTI space coregistration.

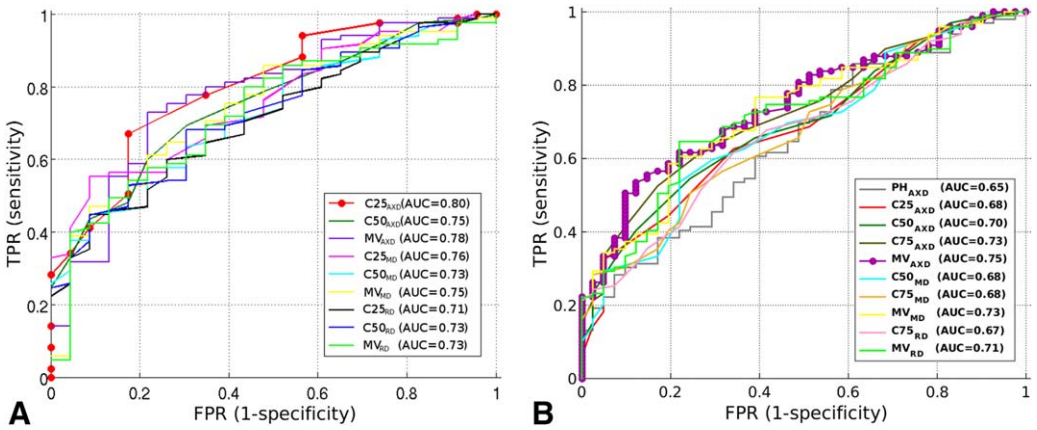

FIGURE 2: ROC curves relative to the comparison of MCI plus AD vs. HS in local cohort dataset (A) and ADNI cohort dataset (B). In these figures, sensitivity is the proportion of MCI and AD patients correctly classified and specificity is the proportion of HS correctly classified. Different features are represented with different colors; the features with maximum AUC are highlighted with colored circles.

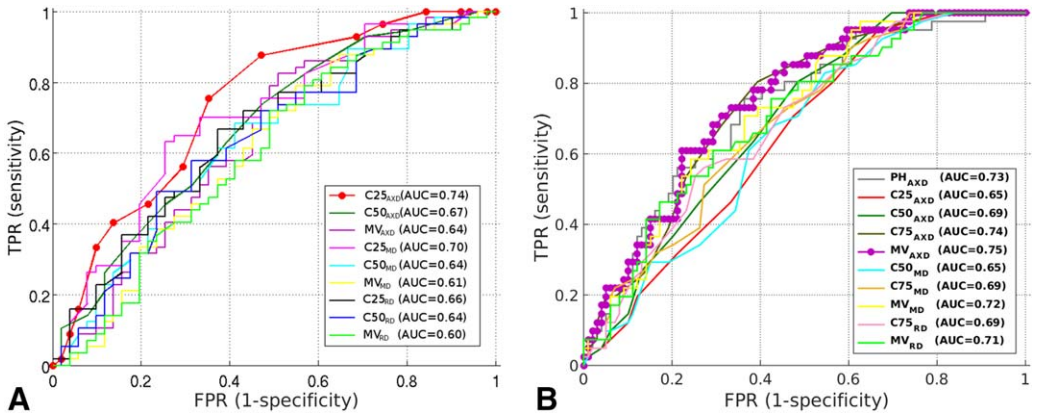

FIGURE 3: ROC curves relative to the comparison AD vs. HS plus MCI in local cohort dataset (A) and ADNI cohort dataset (B). In these figures, sensitivity is the proportion of AD patients correctly classified and specificity is the proportion of HS and MCI subjects correctly classified. Different features are represented with different colors; the features with maximum AUC are highlighted with colored circles.

NAWM masks and anatomical to DTI space warping were carefully checked to assure accuracy. DTI data were acquired with similar but not identical protocols, differing in number of diffusion gradients and spatial resolution. The number of gradients (61 vs. 41) should not substantially influence the DTI diffusivity measures,[30,31] but the in-plane resolution (about 3 times lower in the local dataset) affects the amount of partial volume effects. Comparing the histogram shapes and the range of diffusivity values relative to local and ADNI cohorts with the DTI values referred by the literature[32] confirms this hypothesis, as the histograms of the local cohort dataset (suffering a greater partial volume effect) tend to include more bins with low FA and high diffusivity values. This observation accounts for both the FA histogram not being unimodal and diffusivity histograms having right tails with lower slope when compared to the ADNI ones.

Nevertheless, the results of the two histogram analyses converged in selecting axial diffusivity as the best discriminator, and yielded similar AUC values for $C25_{AXD}$ (for the local cohort dataset) and MV_{AXD} (for the ADNI cohort dataset), therefore indicating a similar group discrimination capability.

WM damage in AD has been interpreted on the basis of two coexisting main pathophysiological mechanisms[33]: neurodegeneration and myelin damage. The former mechanism induces axonal damage caused by Wallerian degeneration,[34] secondary to the effect of cortical neuronal loss. Concurrently, homeostatic repair mechanisms are activated by demyelinating processes, with amyloid and tau accumulating as by-products of these mechanisms. Evidence[34] suggests that in the early stage of the disease these pathological processes coexist and are relatively independent, while at later stages Wallerian degeneration seems to prevail. Reduced AXD and increased RD have been proposed as specific markers of axonal degeneration and demyelination, respectively, based on animal models.[34,35] However, this interpretation in human brain data has been challenged.[36] In particular, little evidence of reduced AXD has been reported, with the majority of studies reporting *increased* AXD in multiple conditions, including AD.[37] A previous study comparing these indices in patients with AD at differing stages[38] showed increased axial diffusivity as the earliest sign of white matter change. They speculated that these changes could reflect early inflammatory events such as microglial activation, which has been implicated in AD pathophysiology.[39] In accordance with these findings, we found in both the local and ADNI datasets an increase of MD, AXD, and RD in the NAWM of patients (MCI, AD—probably driven by the latter) when compared with healthy subjects, while only changes in AXD were able to also distinguish MCI from AD.

The interpretation of increased AXD as a marker of inflammation is very speculative, and alternative explanations are possible, including some form of axonal degeneration. This would fit with the hypothesis of Wallerian degeneration secondary to distal cortical atrophy, as the neuropathological process underlying WM damage in AD, particularly along the main cholinergic pathways. Currently, our data do not allow us to draw a firm conclusion on the substrate of the measured change.

Regardless of the pathological substrate, our data indicate that AXD histogram-derived parameters are the most promising indexes among the ones here investigated for patient stratification. With regard to the potential clinical impact of our study, the results of ROC analyses and post-hoc correlation analysis are promising. Although these results need to be confirmed by further studies on larger patient populations and different MRI scanners and DTI protocols, the ROC analyses results indicate that AXD features in the NAWM have the capability of discriminating between groups, while the post-hoc correlation results highlight that AXD features account for the patients' level of global cognitive impairment, thus expressing the clinical impact of brain involvement. These findings suggest that histogram features of AXD might be reliable biomarkers to be used in clinical trials (ie, patients' staging and follow-up) and, possibly, as a diagnostic tool in clinical settings. In future work, it will be interesting to test if the classification performance, and consequently the clinical usefulness, could be improved by using a linear/nonlinear combination of AXD features and/or exploiting more sophisticated classification algorithms, such as those used in machine learning (eg, Support Vector Machine, Random Forest).

One might argue that neuropsychological assessments provide a comparable performance at a lower cost. However, MRI is typically performed at the time of diagnosis, and current DTI protocols (available on all clinical scanners) would add only a few minutes to the basic clinical protocol. The advantage of imaging biomarkers is that they are more objective and might be more sensitive than MMSE at the very early stages. Clearly, more validation is needed before these tools can be translated into the clinic.

There were some limitations in our study. First, this study lacked longitudinal data. Moreover, data for DTI analysis are relatively easy to acquire; nevertheless, recent development in microstructural imaging suggest that more sophisticated approaches[40] can provide more specific information about WM. Future studies are warranted to investigate whether more accurate biomarkers for AD progression can be obtained by applying histogram analysis to indices derived from these advanced models of diffusion. An important observation is that the spatial resolution of DTI might affect the results of histogram analysis. While further investigations are required, the current recommendation would be

to match the ADNI protocol. Another potential source of bias is the different resolution of T_1-weighted and T_2-weighted data, which were coregistered for the purpose of obtaining the NAWM mask. While ideally one would acquire data with similar geometry, in this case the sequences were optimized for brain segmentation and lesion segmentation, respectively. Regarding lesion segmentation, it is also legitimate to wonder whether, as patients tend to have higher lesion load, this could introduce a bias. However, we excluded participants with lesion volume larger than 25 ml and all histograms were normalized by the total voxel count. This implies that, for every participant, the number of total lesion voxels was at least 20–30 times less than the number of NAWM voxels. Including/excluding in the NAWM histograms such a small amount of voxels would not affect the shape of the histograms, which would be substantially unchanged.

Finally, it should be noted that the local cohort groups were well matched for age and gender, but the level of education was higher in healthy controls compared to the patients' groups (education is not available for the ADNI cohort). While this may introduce a potential bias, it is a fairly common occurrence in this kind of study.

In conclusion, our findings suggest that histogram-derived measures of AXD in NAWM might be a sensitive marker of microstructural brain tissue changes occurring during the course of AD and might be useful to predict the rate of disease progression, and hopefully to be used as an index of response to medication in pharmacological trials.

Acknowledgment

Contract grant sponsor: Italian Ministry of Health; contract grant number: RF09.150; RF10.047 (to M.B.).

References

1. Petersen RC, Aisen P, Boeve BF, et al. Criteria for mild cognitive impairment due to Alzheimer's disease in the community. Ann Neurol 2013;74:199–208.
2. Dubois B, Feldman HH, Jacova C, et al. Revising the definition of Alzheimer's disease: a new lexicon. Lancet Neurol 2010;9:1118–1127.
3. Vemuri P, Whitwell JL, Kantarci K, et al. Antemortem MRI based STructural Abnormality iNDex (STAND)-scores correlate with postmortem Braak neurofibrillary tangle stage. Neuroimage 2008;42:559–567.
4. Patwardhan MB, McCrory DC, Matchar DB, Samsa GP, Rutschmannet OT. Alzheimer disease: operating characteristics of PET. A meta-analysis. Radiology 2004;231:73–80.
5. Ikonomovic MD, Klunk WE, Abrahamson EE, et al. Post-mortem correlates of in vivo PiB-PET amyloid imaging in a typical case of Alzheimer's disease. Brain 2008;131:1630–1645.
6. Fortea J, Vilaplana E, Alcolea D, et al. Cerebrospinal fluid β-amyloid and phosphor-tau biomarker interactions affecting brain structure in preclinical Alzheimer disease. Ann Neurol 2014;76:223–230.
7. Frisoni GB, Fox NC, Jack CR, et al. The clinical use of structural MRI in Alzheimer disease. Nat Rev Neurol 2010;6:67–77.
8. Caso F, Agosta F, Filippi M. Insights into white matter damage in Alzheimer's disease: from postmortem to in vivo diffusion tensor MRI studies. Neurodegen Dis 2016;16:26–33.
9. Tournier JD, Mori S, Leemans A. Diffusion tensor imaging and beyond. Magn Reson Med 2011;65:1532–1556.
10. Bosch B, Arenaza-Urquijo EM, Rami L, et al. Multiple DTI index analysis in normal aging, amnestic MCI and AD. Relationship with neuropsychological performance. Neurobiol Aging 2012;33:61–74.
11. Holtmannspötter M, Peters N, Opherk C, et al. Diffusion magnetic resonance histograms as a surrogate marker and predictor of disease progression in CADASIL: a two-year follow-up study. Stroke 2005;36: 2559–2565.
12. Steffen–Smith EA, Sarlls JE, Pierpaoli C, et al. Diffusion tensor histogram analysis of pediatric diffuse intrinsic pontine glioma. Biomed Res Int 2014:647356.
13. Lema A, Bishop C, Malik O, et al. A comparison of magnetization transfer methods to assess brain and cervical cord microstructure in multiple sclerosis. J Neuroimaging 2017;27:221–226.
14. McKhann GM, Knopman DS, Chertkow H, et al. The diagnosis of dementia due to Alzheimer's disease: recommendations from the National Institute on Aging-Alzheimer's Association workgroups on diagnostic guidelines for Alzheimer's disease. Alzheimers Dement 2011;7:263–269.
15. American Psychiatric Association. Diagnostic and statistical manual of mental disorders, 5th ed. Arlington, VA: American Psychiatric Association Publishing; 2013.
16. Hughes CP, Berg L, Danziger WL, Coben LA, Martin RL. A new clinical scale for the staging of dementia. Br J Psychiatry 1982;140: 566–572.
17. Hachinski VC, Iliff LD, Zilhka E, et al. Cerebral blood flow in dementia. Arch Neurol 1975;32:632–637.
18. Iadecola C. The pathobiology of vascular dementia. Neuron 2013;80: 844–866.
19. Büsch D, Hagemann N, Bender N. The dimensionality of the Edinburgh Handedness Inventory: An analysis with models of the item response theory. Laterality 2010;15:610–628.
20. Barletta-Rodolfi C, Gasparin F, Ghidoni E. Kit del neuropsicologo italiano. Milan, Italy: Dynamicom Edizioni, 2011.
21. Orsini A, Grossi D, Capitani E, Laiacona M, Papagno C, Vallar G. Verbal and spatial immediate memory span: Normative data from 1355 adults and 1112 children. Ital J Neurol Sci 1987;8:539–548.
22. Miceli G, Laudanna A, Burani C, et al. Batteria per l'analisi dei deficit afasici. Associazione per lo sviluppo delle ricerche neuropsicologiche. Milan, Italy: Berdata; 1991.
23. Folstein MF, Folstein SE, McHugh PR. Mini-mental state. A practical method for grading the cognitive state of patients for the clinician. J Psychiatr Res 1975;12:189–198.
24. Avants BB, Tustison NJ, Song G, et al. A reproducible evaluation of ANTs similarity metric performance in brain image registration. Neuroimage 2011;54:2033–2044.
25. Leemans A, Jones DK. The B-matrix must be rotated when correcting for subject motion in DTI data. Magn Reson Med 2009;61:1336–1349.
26. Tofts PS, Davies GR, Dehmeshki J. Histograms: Measuring subtle diffuse disease. In: Tofts P, editor. Quantitative MRI of the brain: Measuring changes caused by disease. Chichester, UK; John Wiley & Sons; 2003:581–610.
27. Fawcett T. An introduction to ROC analysis. Pattern Recogn Lett 2006;27:861–874.
28. Hua X, Hibar DP, Ching CR, et al. Unbiased tensor-based morphometry: improved robustness and sample size estimates for Alzheimer's disease clinical trials. Neuroimage 2013;66:648–661.
29. Cercignani M. Strategies for patient-control comparison of diffusion MR Data. In: Jones DK, editor. Diffusion MRI: Theory, methods, and applications. Oxford, UK: Oxford University Press; 2010:485–499.

30. Lebel C, Benner T, Beaulieu C. Six is enough? Comparison of diffusion parameters measured using six or more diffusion-encoding gradient directions with deterministic tractography. Magn Reson Med 2012;68:474–483.

31. Zhan L, Leow AD, Jahanshad N, et al. How does angular resolution affect diffusion imaging measures? Neuroimage 2010;49: 1357–1371.

32. Palacios EM, Martin AJ, Boss MA, et al. Toward precision and reproducibility of diffusion tensor imaging: a multicenter diffusion phantom and traveling volunteer study. AJNR 2017;38:537–545.

33. O'Dwyer L, Lamberton F, Bokde ALW, et al. Using diffusion tensor imaging and mixed-effects models to investigate primary and secondary white matter degeneration in Alzheimer's disease and mild cognitive impairment. J Alzheimers Dis 2011;26:667–682.

34. Amlien IK, Fjell AM. Diffusion tensor imaging of white matter degeneration in Alzheimer's disease and mild cognitive impairment. Neuroscience 2014;276:206–215.

35. Song SK, Sun SW, Ramsbottom MJ, et al. Dysmyelination revealed through MRI as increased radial (but unchanged axial) diffusion of water. Neuroimage 2002;17:1429–1436.

36. Wheeler-Kingshott CA, Cercignani M. About "axial" and "radial" diffusivities. Magn Reson Med 2009;61:1255–1260.

37. Acosta-Cabronero J, Nestor PJ. Diffusion tensor imaging in Alzheimer's disease: insights into the limbic-diencephalic network and methodological considerations. Front Aging Neurosci 2014;6:266.

38. Acosta-Cabronero J, Alley S, Williams GB, et al. Diffusion tensor metrics as biomarkers in Alzheimer's disease. PLoS One 2012;7: e49072.

39. Bagyinszky E, Giau VV, Shim K, et al. Role of inflammatory molecules in the Alzheimer's disease progression and diagnosis.. J Neurol Sci 2017;376:242–254.

40. Zhang H, Schneider T, Wheeler-Kingshott CA, Alexander DC. NODDI; practical in vivo neurite orientation dispersion and density imaging of the human brain. Neuroimage 2012;61:1000–1016.